IJIREEICE ISSN (O) 2321-2004, ISSN (P) 2321-5526

International Journal of Innovative Research in Electrical, Electronics, Instrumentation and Control Engineering

Impact Factor 7.047 ⁜ Vol. 10, Issue 3, March 2022

DOI: 10.17148/IJIREEICE.2022.10311

Cost Minimization of Charging Stations Using PV Array

Anmol Dureja[1], Anshita Pandit[2], Sagar Bharti[3] ,Poonam Juneja[4]

Student, EEE Department, MAIT, Rohini, Delhi, India[1]

Student, EEE Department, MAIT, Rohini, Delhi, India[2]

Student, EEE Department, MAIT, Rohini, Delhi, India[3]

Asst. Professor, EEE Department, MAIT, Rohini, Delhi, India[4]

Abstract: India is currently the third largest energy consuming country in the world. And it meets a majority of these humongous needs for energy by conventional non-renewable sources of energy. But, progress is being made to apply more renewables in the energy production sector. One such place is the EV market where the government is introducing great incentives to encourage people to buy more eco-friendly means of transportation. Now, the biggest barrier to wide-scale adaptability of EV is the lack of infrastructure. Compared to several petrol pumps for every kilometer of road, electric charging stations are a rare sight. We discuss a system to fix both of these problems by using renewables to power charging stations decreasing the. The system uses photovoltaic solar panels to charge EV batteries and also supply excess energy to the grid during peak sunshine hours thereby covering its cost of installation and maintenance relatively quicker than conventional solar power setups. A sepic converter is used for dc-dc conversion and a line commutated converter is preferred to act as both rectifier and inverter using a bidirectional configurator. This system has been simulated in Simulink and resultant responses have also been shown in the paper.

Keywords: Photovoltaic panels, Electric Vehicle, Renewable Energy, Bidirectional configurator, Cost minimization

I.INTRODUCTION

In recent years, there has been a greater focus on the devastating effects of climate change and how carbon emissions play a key part in this. When you consider that the country is the third most polluted in the world [1], it appears that now is a fantastic time for the general public to switch to electric vehicles. However, there are still a few roadblocks to overcome before EVs become widely used and extensive research is being conducted on the same [2-4]. The most serious issue is a charging infrastructure that is essentially non-existent. This study investigates a charging station that is fueled by solar energy during regular and peak sunlight hours and consumes energy directly from the grid during the rest of the time. The following approach is used to reduce the cost of such charging stations. Less units will be consumed during peak sunshine hours, when demand is high and unit price is likewise high, and excess power generated will be delivered to the power system. When demand is low, power from the grid can be used to charge the vehicle, accelerating the charging station's cost recovery. Because it can operate in boost and buck modes and does not change the polarity of the incoming signal, the system described above requires a sepic converter to maintain a consistent voltage supply to the battery [5-7]. To connect the system to the power supply, a line commutated converter with a bidirectional configurator is utilized [8].

II.COMPONENTS USED

As illustrated in Fig. 1, the proposed EV battery charger includes a PV array, a sepic converter, a Line commutated converter, a bi - directional configurator, an electric vehicle battery, a single phase utility grid, relays, and a controller. Each of the blocks represented in Fig. 1 is described in the sub-sections below.

IJIREEICE ISSN (O) 2321-2004, ISSN (P) 2321-5526
International Journal of Innovative Research in Electrical, Electronics, Instrumentation and Control Engineering
Impact Factor 7.047 ⁜ Vol. 10, Issue 3, March 2022
DOI: 10.17148/IJIREEICE.2022.10311

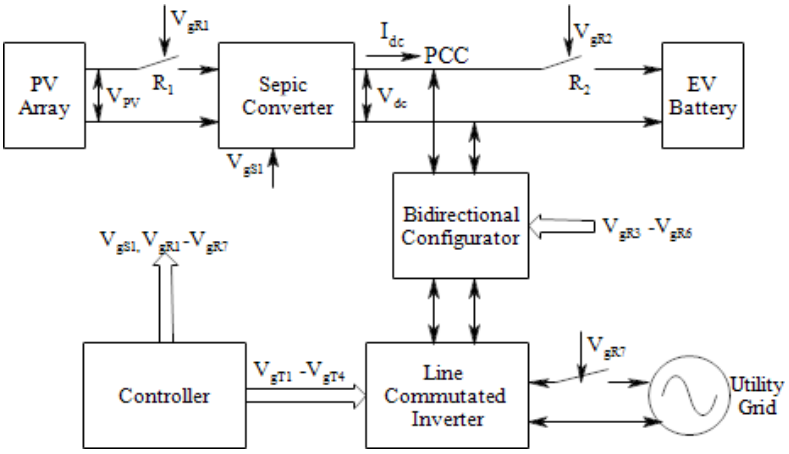

Fig.1 Block Diagram of the EV Battery Charger

1. Line Commutated Converter

The Line Commutated Converter is made up of four SCR switches and a dc link inductor, Ldc, that has an internal resistance of Rdc. If Vdc > Edc, LCC runs in inverter mode to feed power to the grid from the PV array when α > 90°. During α< 90°, on the other hand, the LCC operates in rectifier mode, reversing the polarity of the dc link voltage, Edc, necessitating the reversal of the polarity of Vdc for supplying power from the grid to the EV battery. The suggested bidirectional configurator, which is described in the following section, accomplishes this.
The dc link voltage of LCC, E_{dc} is given by [9]

$$E_{dc}=(2V_m/p)\cos\alpha \quad (1)$$

Where, V_m is the peak amplitude of ac voltage and α is the firing angle of SCR switches.

The dc link inductance, L_{dc} is designed for continuous conduction using the following equation

$$L_{dc\text{-}critical}=E_{dc}/I_{dclink} \quad (2)$$

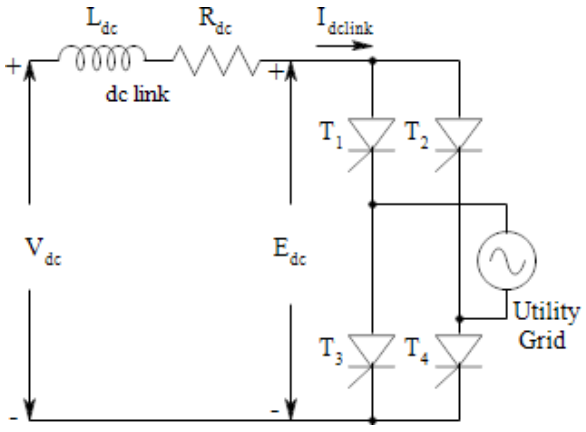

Fig.2 Circuit diagram of Line commutated converter configured as inverter

2. Bidirectional Configurator

As illustrated in Fig.3, the suggested bidirectional configurator consists of four relays that are positioned in such a way that LCC functions as a bidirectional ac-dc converter. In inverter mode, this bidirectional configurator ensures the bidirectional flow of power from PCC to grid, and in rectifier mode, it ensures the bidirectional flow of power from grid to PCC. Relays R3 and R4 are closed during inverter mode to connect point 'A' of PCC to point 'C' of dc link and point

IJIREEICE ISSN (O) 2321-2004, ISSN (P) 2321-5526
International Journal of Innovative Research in Electrical, Electronics, Instrumentation and Control Engineering
Impact Factor 7.047 ⁜ Vol. 10, Issue 3, March 2022
DOI: 10.17148/IJIREEICE.2022.10311

'B' of PCC to point 'D' of dc link, respectively. Relays R5 and R6 remain open in this mode, as indicated in Fig. 4. (a). As mentioned in sub-section III.I, the polarity of Vdc must be reversed during rectifier mode, so point 'A' is connected to point 'D' and point 'B' is connected to point 'C' by closing relays R5 and R6 respectively while opening relays R3 and R4 as shown in Fig. 4(b) to ensure EV battery charging from utility grid during this mode.

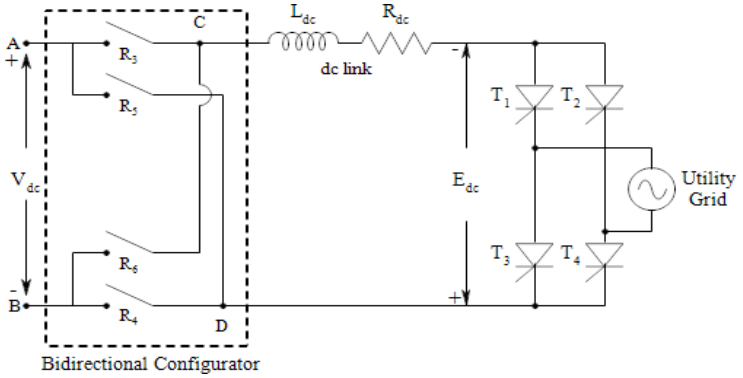

Fig.3. Schematic diagram of Bidirectional Configurator

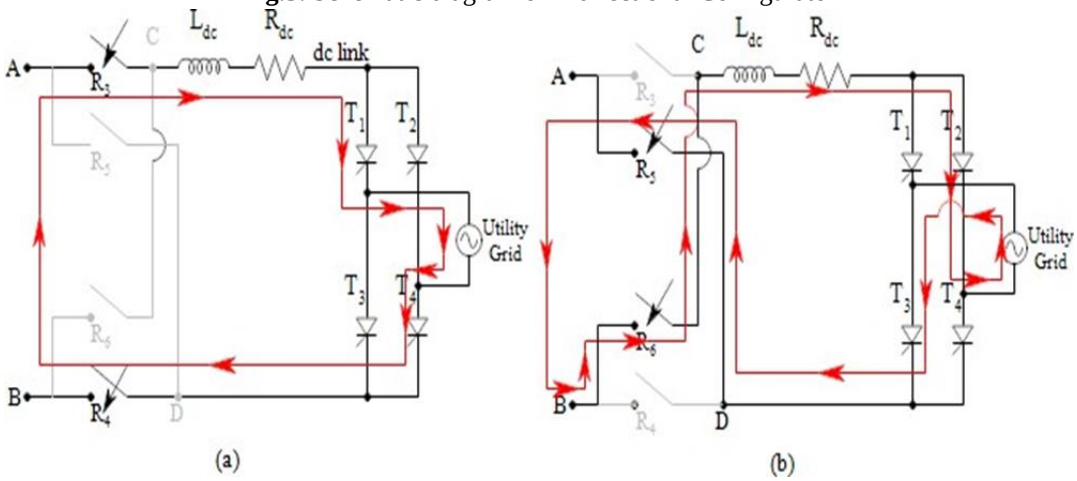

Fig.4. Schematic diagram of LCC configured as (a)inverter & (b)rectifier

3. Sepic Converter

A single-ended primary-inductor converter, or SEPIC converter, is a type of converter that steps up or steps down the input voltage using a boost control topology. As shown in Fig.5, the proposed system consists of one IGBT switch, one diode, two inductors, and two capacitors. The PI controller is used to adjust the duty cycle of the sepic converter in order to provide a constant output voltage charging method. The voltage supplied by the sepic converter is as follows: [10]

$$V_{dc}/V_{pv}=\delta/1-\delta \quad (3)$$

Where, δ is the duty cycle of sepic converter, Vpv is the PV array voltage. The inductors and capacitors of sepic converter are designed as per the equations below:

$$L_a=L_b=V_{pv\ min}\ \max\ \delta/2\Delta i_{pv}f_s \quad (4)$$

$$C_1=I_{dc}\delta_{max}/\Delta V_{C1}f_s \quad (5)$$

$$C_2=I_{dc}\delta_{max}/\Delta V_{dc}f_s \quad (6)$$

Where, V_{pvmin} is the minimum PV array voltage, Δi_{PV} is the input current ripple, f_s is the switching frequency, I_{dc} is the current flowing through the PCC, ΔV_{C1} is the capacitor, C_1 voltage ripple, ΔV_{dc} is the output voltage ripple, and δ_{max} is the maximum duty cycle which is given by

IJIREEICE ISSN (O) 2321-2004, ISSN (P) 2321-5526
International Journal of Innovative Research in Electrical, Electronics, Instrumentation and Control Engineering
Impact Factor 7.047 ⁜ Vol. 10, Issue 3, March 2022
DOI: 10.17148/IJIREEICE.2022.10311

$$\delta_{max} = \frac{V_{dc} + V_D}{V_{PVmin} + V_{dc} + V_D}$$

where, V_d is the voltage drop.

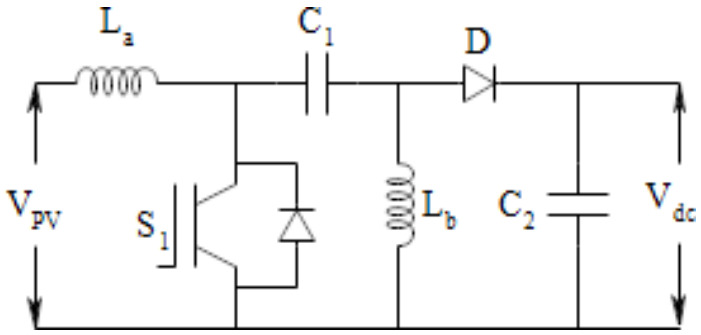

Fig.5. Circuit Diagram of sepic converter

4. Controller

In the proposed system, the controller generates gate pulses for the sepic converter, LCC, bidirectional configurator, and additional relays. A PI controller is designed to generate gate pulses to the sepic converter switch by varying the duty cycle to maintain constant voltage at the PCC regardless of solar irradiation. To operate the LCC in inverter mode and feed the PV array power to the utility grid during peak sun-shine hours or full charge condition of the EV battery, firing pulses to the SCR switches of the LCC are generated with $\alpha > 90°$.

III. WORKING

Working of the proposed system is explained in 4 different modes of operation depending on the solar irradiation conditions and SOC of EV battery viz (i) mode 1 (P-V), (ii) mode 2 (P-VG), (iii) mode 3 (G-V) and (iv) mode 4 (P-G).

Mode 1: Forward PV-EV battery charging mode (P-V)

In this mode, the solar power generated is sufficient to charge only the EV battery during normal sunlight hours. The relays R1 and R2 are closed during this mode to transfer power from the PV array to the EV battery. Other relays in bidirectional configurator R3-R6 and relay R7 are open, effectively disconnecting the LCC and utility grid from the system.

Mode 2: Forward PV- EV battery & Grid mode (P-VG)

In this mode, excess power generated by the PV array is fed to the utility grid rather than just charging the EV battery. To transfer PV array power to the EV battery and the grid, relays R1, R2, and R7 are closed, in addition to bi - directional configurator relays R3 and R4, to configure the LCC as a line commutated inverter (LCI), as shown in Fig. 3.

Mode 3: Reverse grid- EV battery charging mode (G-V)

Solar power generated is insufficient to charge the EV battery during low sunlight hours and at night. As a result, with relays R2 and R7 closed, grid power is used to charge the EV battery. R5 & R6 relays in the bidirectional configurator are closed to configure LCC as a rectifier in this mode, allowing power to be transferred from the utility grid to the EV battery. In this mode, the PV array was isolated from the intended charging system by opening Relay R1.

Mode 4: PV- grid mode (P-G)

When an EV battery is fully charged, it must be disconnected from the charging system, and the solar energy generated

IJIREEICE ISSN (O) 2321-2004, ISSN (P) 2321-5526
International Journal of Innovative Research in Electrical, Electronics, Instrumentation and Control Engineering
Impact Factor 7.047 ⁜ Vol. 10, Issue 3, March 2022
DOI: 10.17148/IJIREEICE.2022.10311

is fed directly to the grid in mode 4. Except for the opening of relay R2 to separate the EV battery from the proposed system, the activities of the relays are the same as in mode 2.
The next section explains the detailed operation of the controller, which is essential to the operation of the proposed charging system in various modes of operation.

Controller

In the Line commutated converter, the proposed system's controller generates gate pulses to the sepic converter switch and firing pulses to the SCR switches. It also controls the relays R1, R2, R7, as well as the relays in the bidirectional configurator R3, R4, R5, and R6, based on the PV array irradiation conditions, where (i) PL is the low PV array power generated at the specified lower irradiation limit, and (ii) PU is the PV array power generated at the specified upper irradiation limit. Table 1 shows the operating conditions of bidirectional configurator relays and other relays in the proposed system for various modes of operation.

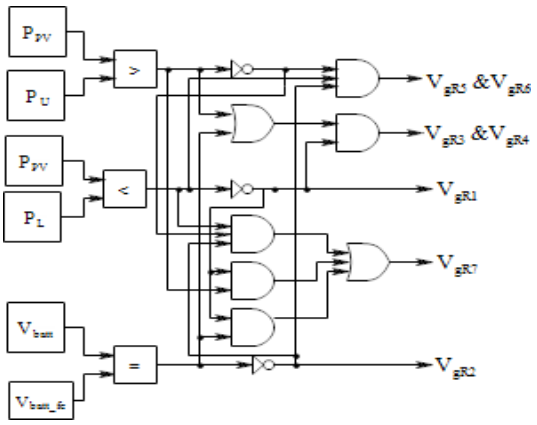

(a)

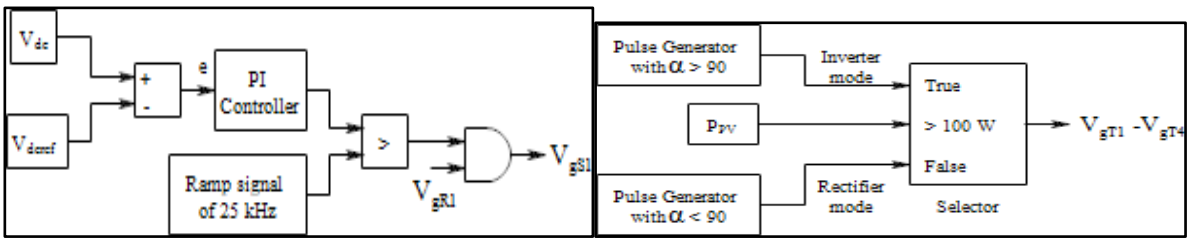

(b) (c)

Fig.6. Schematic diagram of (a) Relay controller (b) Sepic converter controller and (c) LCC controller

PV array with SEPIC converter is linked to EV battery alone during P_L <PPV ≤ PU by closing relays R1 and R2. By keeping relays R3, R4, R5, and R6 in bidirectional configurator and relay R7 in open state, the charging system is unplugged from the grid. Control signals are created during PPV > PU to close the relays R1, R2, and R7 in the bidirectional configuration, as well as relays R3 and R4, to charge the EV battery and transfer surplus power to the grid. During PPV <PL, the PV array is disconnected from the charging system by opening relay R1, and the EV battery is charged from utility grid power by shutting relays R5 & R6 and opening relays R3 & R4 in a bidirectional configurator with relay R7 closed.

When the EV battery is fully charged, the battery voltage reaches its full charge voltage, Vbatt-fc, at which point the charging system is unplugged by opening the relay R2. Figure 1 depicts the generation of control signals for operating relays as shown in Fig. 6(a). As shown in Fig. 6(b), the PI controller generates gate pulses to the sepic converter's MOSFET switch to maintain a constant voltage at PCC by varying the duty cycle of the gate pulses based on the PV array voltage.

IJIREEICE ISSN (O) 2321-2004, ISSN (P) 2321-5526

International Journal of Innovative Research in Electrical, Electronics, Instrumentation and Control Engineering

Impact Factor 7.047 ⁜ Vol. 10, Issue 3, March 2022

DOI: 10.17148/IJIREEICE.2022.10311

Also, the controller generates firing pulses to the LCC depending on the PV array generated power. If $P_{PV} > P_U$, controller generates firing pulse with $\alpha > 90°$ to SCR switches T_1 and T_4 and to the switches T_2 and T_3 with 180° phase shifted from that of the T_1& T_4 firing pulse to operate LCC in forward inverter mode for feeding the excess PV array power to the single-phase utility grid. If $P_{PV} < P_L$, controller generate firing pulse with $\alpha < 90°$ to switches T_2 and T_3 and firing pulse to the switches T_1 and T_4 are provided with 180° phase shift from that of T_2 and T_3 firing pulses to operate LCC in reverse rectifier mode to charge EV battery from single phase utility grid as shown in Fig. 6(c).

Table.1 Operation of relays in the proposed system

Modes	Irradiation Condition	EV Battery SOC	Relays			Bidirectional Configurator Relays	
			R_1	R_2	R_7	R_3 & R_4	R_5 & R_6
P-V	$P_L < P_{PV} \leq P_U$	0	1	1	0	0	0
P-VG	$P_{PV} > P_U$	0	1	1	1	1	0
G-V	$P_{PV} < P_L$	0	0	1	1	0	1
P-G	$P_{PV} > P_L$	1	1	0	1	1	0
Null	$P_{PV} < P_L$	1	0	0	0	0	0

IV. RESULTS AND DISCUSSION

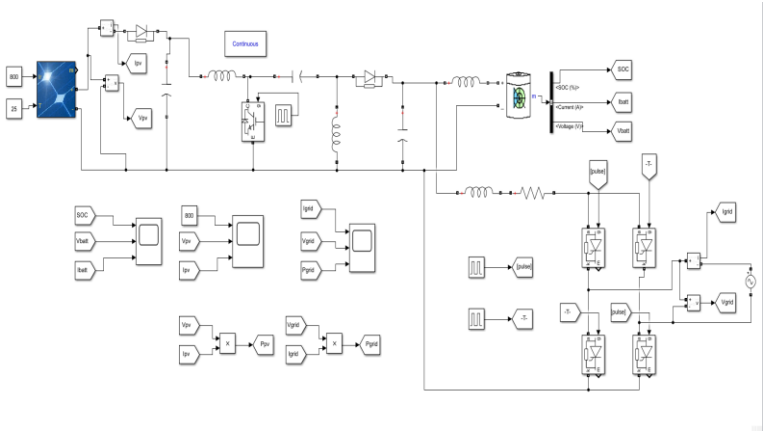

Fig.7. Simulation model of proposed EV battery charger

The dynamic response of the system was studied using the developed simulation model for 500 W/m2, 800 W/m2, and 100 W/m2 PV array irradiation in modes 1: (P-V), mode 2: (P-VG), and mode 3: (G-V), respectively. Figure 8 depicts the modeling results for PV array voltage, VPV and current, IPV waveforms, and solar irradiation in all three modes. Figure 9 depicts the EV battery SOC, battery voltage, Vbatt and current, Ibatt waveforms. Figure 10 shows the LCC's dc link voltage, Edc, and current, Idclink, as well as the grid voltage, Vgrid, and current, Igrid.

IJIREEICE ISSN (O) 2321-2004, ISSN (P) 2321-5526
International Journal of Innovative Research in Electrical, Electronics, Instrumentation and Control Engineering
Impact Factor 7.047 ⁜ Vol. 10, Issue 3, March 2022
DOI: 10.17148/IJIREEICE.2022.10311

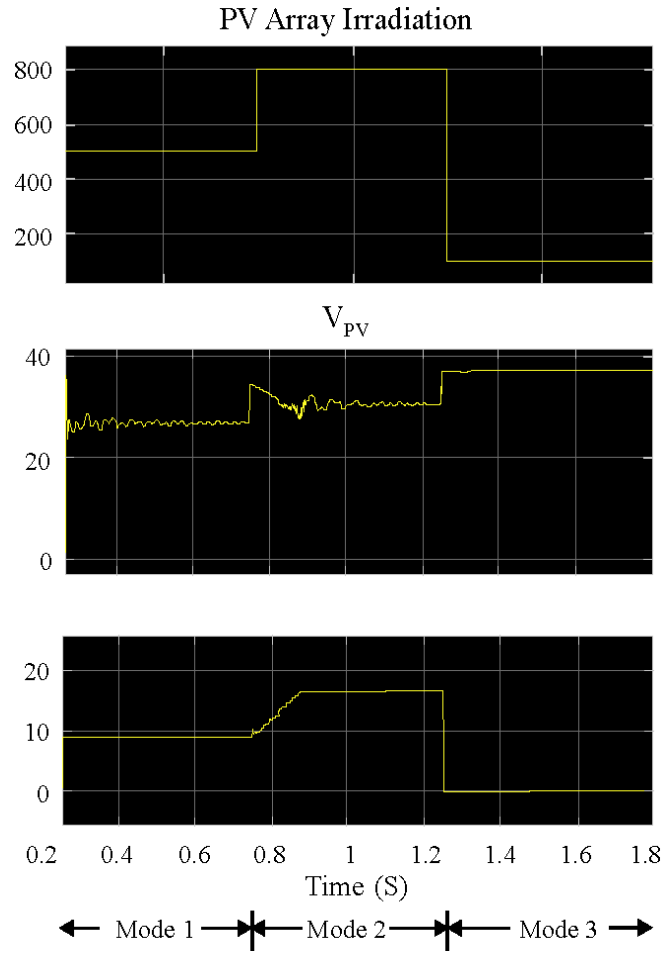

Fig.8. Waveforms of PV array irradiation, PV array voltage, V_{PV} and PV array current, I_{PV}

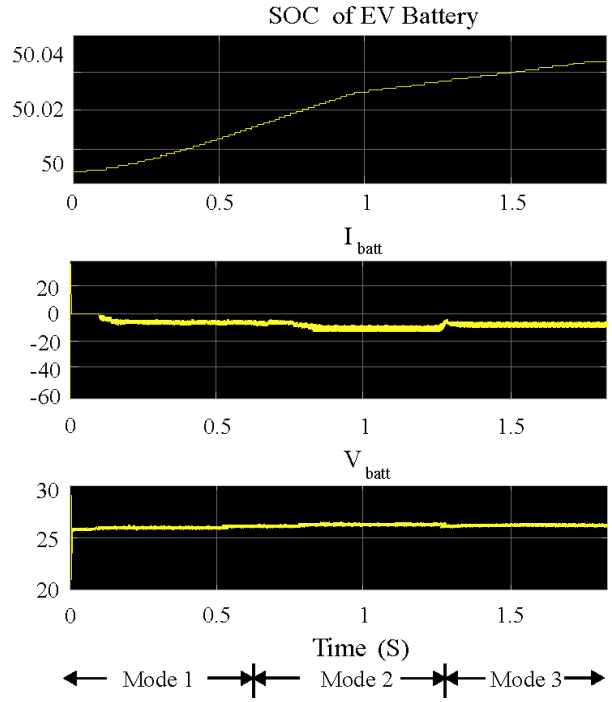

Fig.9. Waveforms of EV battery SOC, Voltage, I_{batt} and current V_{batt}

IJIREEICE ISSN (O) 2321-2004, ISSN (P) 2321-5526
International Journal of Innovative Research in Electrical, Electronics, Instrumentation and Control Engineering
Impact Factor 7.047 ⁜ Vol. 10, Issue 3, March 2022
DOI: 10.17148/IJIREEICE.2022.10311

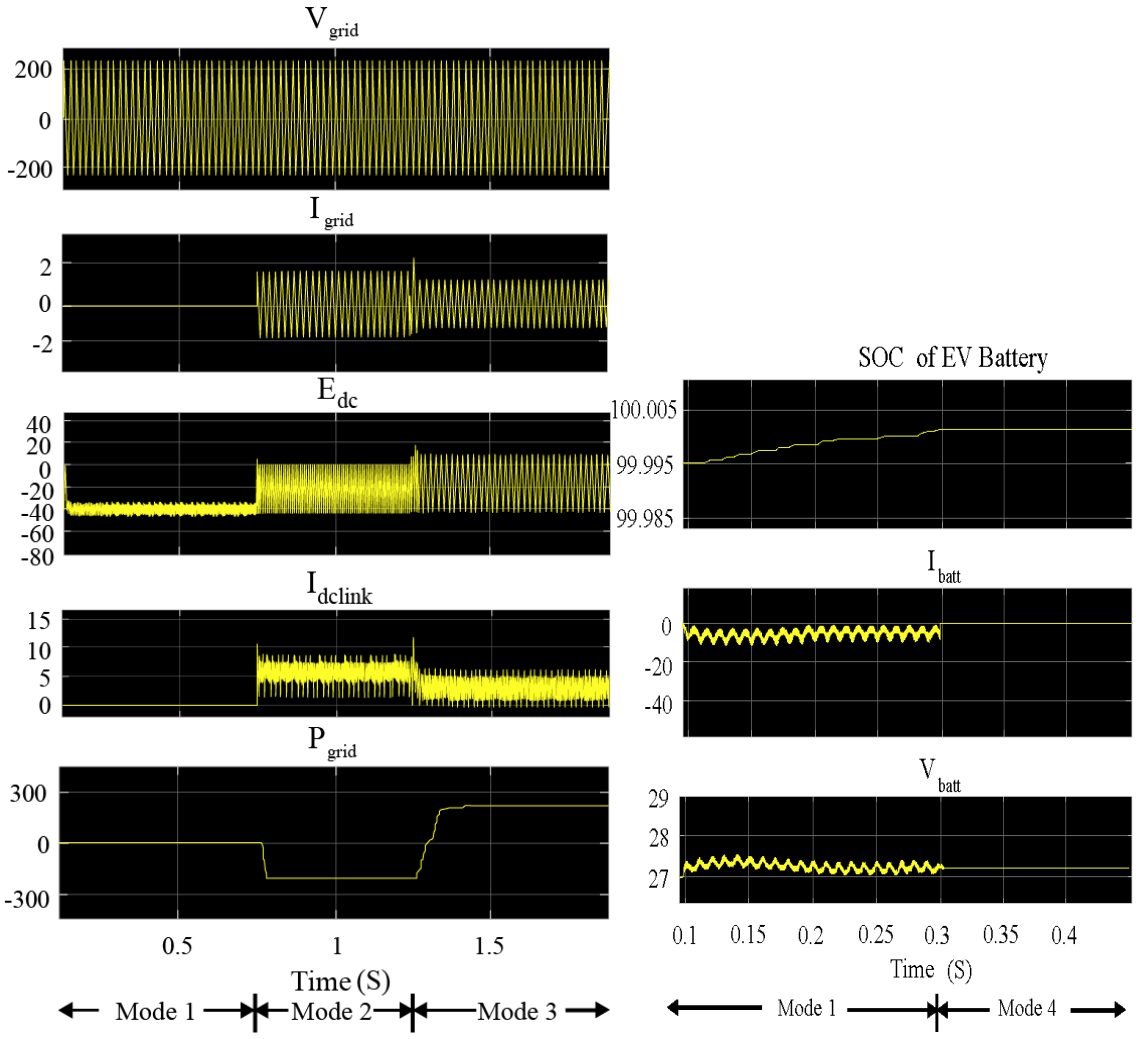

Fig.10. Dynamic response of EV battery waveforms from Mode 1 to Mode 4

In mode 1, the PV array voltage of 31.64 V and current of 7.27 A contributing to the power of 230 W is step down to a voltage of 26.64 V and current of 8.169 A by the sepic converter to charge the EV battery alone because the PV array generated power is sufficient to charge the EV battery alone, as shown in Fig. 8, 9 and 10. The proposed charging system is separated from the grid in this mode, as shown by the grid current of 0 A in Fig. 10.

In mode 2, the PV array voltage of 34.6 V and current of 13.58 A is bucked to a constant voltage of 26.7 V and current of 16.53 A at the sepic output terminal, which is delivered to both the EV battery and the grid. In this mode, LCC runs in inverter mode with a constant firing angle of $\alpha = 120°$, resulting in a negative dc link voltage, Edc, which is less than the voltage at PCC of 26.7 V, ensuring that the power is delivered to the grid via a 1:5 turns ratio step-up transformer. At a current of 0.919 A, 208 W of power is delivered to a single phase 230 V grid. The EV battery is charged in this mode as well, with a battery voltage of 26.6 V and current of 8.2 A.

PV array power is inadequate to charge the EV battery in mode 3, thus the PV array is disconnected from the charging system, as indicated by the increase in PV array voltage to its open circuit value of 37.8 V and a reduction in current to 0 A. In this mode, the EV battery is charged from grid power by using an LCC as a rectifier with a firing angle of $\alpha = 30°$, as represented by the positive Edc in Fig. 10. The increase in SOC and negative battery current in all three modes,

IJIREEICE ISSN (O) 2321-2004, ISSN (P) 2321-5526
International Journal of Innovative Research in Electrical, Electronics, Instrumentation and Control Engineering
Impact Factor 7.047 ⁜ Vol. 10, Issue 3, March 2022
DOI: 10.17148/IJIREEICE.2022.10311

regardless of solar irradiation circumstances, indicates that the EV battery is charged, as shown by the increase in SOC and negative battery current in Fig. 9.

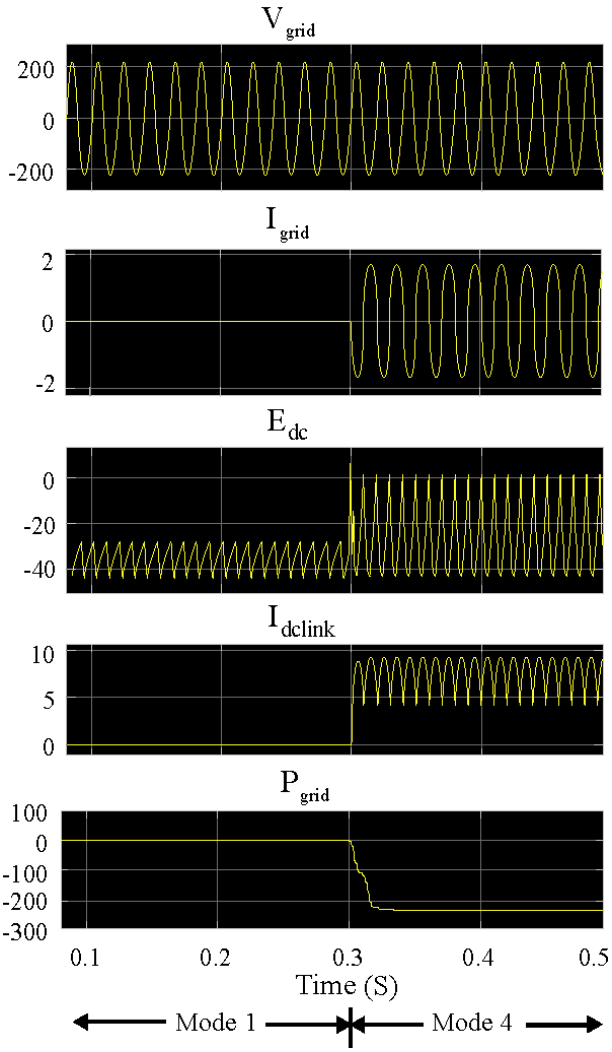

Fig.11 Dynamic response of grid voltage & current and dc bus voltage & current waveforms from Mode 1 to Mode 4

When the SOC of an EV battery approaches 100%, the charging system's dynamic response is observed as a switch from mode 1 to mode 4. At a 500 W/m2 irradiation, the EV battery is charged only from PV array generated power, and the charging system is disconnected from the grid. If the EV battery's SOC reaches 100 percent in this mode, the charger is turned off, as shown in Fig. 11 by the constant fully charged battery voltage of 27.4 V and zero battery current. In addition, the PV array generated power is fed to the grid, as shown in Fig. 11 by the negative grid power, Pgrid. Table 2 shows a comparison of input and output parameter values in four different modes of operation for the proposed EV battery charger.

Table 2. Comparative results in 4 modes of operation

Parameters	P-V mode	P-VG mode	G -V mode	P-G mode
Irradiation (W/m^2)	500	800	100	500
V_{PV} (V)	31.64	34.6	35.2	31.64
I_{PV} (A)	7.27	13.58	0	7.27

IJIREEICE ISSN (O) 2321-2004, ISSN (P) 2321-5526

International Journal of Innovative Research in Electrical, Electronics, Instrumentation and Control Engineering

Impact Factor 7.047 ⁜ Vol. 10, Issue 3, March 2022

DOI: 10.17148/IJIREEICE.2022.10311

Parameters	P-V mode	P-VG mode	G -V mode	P-G mode
P_{PV} (W)	230	469.8	0	230
V_{dc} (V)	27.74	26.7	26.2	27.74
I_{dc} (A)	8.169	16.53	7.76	8.169
V_{batt} (V)	26.64	26.6	26	27.4
I_{batt} (A)	8.169	8.2	7.76	0
P_{batt} (W)	217.62	218.12	202	0
V_{grid} (V)	230	230	230	230
I_{grid} (A)	0	0.979	0.95	0.95
P_{grid} (W)	0	208	217	217

V. CONCLUSION

The ability of the system to provide uninterruptible charging of an EV battery using the constant voltage charging method, regardless of irradiation circumstances, is discussed in this study. With the help of a bidirectional configuration, the suggested system can charge an EV battery and supply energy to the grid during peak sun-shine hours, and the EV battery can also be charged from the grid during low and non-sun-shine hours. The proposed charging system is built and simulated in the MATLAB software program's Simulink environment, with dynamic effects provided for the four modes of operation. The simulation results reported in this research highlight the proposed charger's effectiveness.

VI. REFERENCES

[1] Air quality in India, www.iqair.com/in-en/india.

[2] Jung, Won & Ismail, Azianti & Ariffin, Mohd Faris & Noor, S. (2011). Study Of Electric Vehicle Battery Reliability Improvement. International Journal of Reliability and Applications. 12. 123-129.

[3] Khurana, A., Kumar, V. V. R., & Sidhpuria, M. (2020). A Study on the Adoption of Electric Vehicles in India: The Mediating Role of Attitude. Vision, 24(1), 23–34. https://doi.org/10.1177/0972262919875548

[4] C Iclodean1 , B Varga, N Burnete, D Cimerdean & B Jurchiș. Comparison of Different Battery Types for Electric Vehicles. (n.d). C Iclodean et al 2017 IOP Conf. Ser.: Mater. Sci. Eng. 252 012058

[5] Abdelhakim BELKAID, Ilhami COLAK, Korhan KAYISLI, Ramazan BAYINDIR, "Design and Implementation of a Cuk Converter Controlled by a Direct Duty Cycle INC-MPPT in PV Battery System", Internatıonal Journal of Smart Grıd, vol.3(1), pp.19-25, 2019

[6] D. Gueye, A. Ndiaye, M. Abdou Tankari, M. Faye, A. Thiam, L. Thiaw, G. Lefebvre, "Design Methodology of Novel PID for Efficient Integration of PV Power to Electrical Distributed Network", International Journal of Smart Grid, vol. 2(1), pp. 77-86, 2018.

[7] Mahdavi M, Farzanehfard H., "Bridgeless SEPIC PFC rectifier with reduced components and conduction losses", IEEE Trans Ind Electron, vol. 58(9), pp. 4153- 4160, 2011.

[8] S. Krithiga, N. Ammasai Gounden, "Investigations of an improved PV system topology using multilevel boost converter and line commutated inverter with solutions to grid issues", Simulation Modelling Practice and Theory, vol. 42, pp. 147-159, 2014.

[9] Krithiga S., D.R.B.B. Jose, H.R. Upadhya, N.A. Gounden, "Grid-Tied Photovoltaic Array Using Power Electronic Converters with Fuzzy Logic Controller for Maximum Power Point Tracking", Australian Journal of Electrical and Electronics Engineering, vol. 9 (4), pp. 393-400, 2012.

[10] Jeff Falin. "Designing DC/DC converters based on SEPIC topology", Analog Applications Journal, 2008.